Opto-Electronic Engineering
光 电 工 程

Review

2022 年, 第 49 卷, 第 5 期

DOI: 10.12086/oee.2022.210407

湿法有机电致发光器件：结构、器件物理及制备工艺

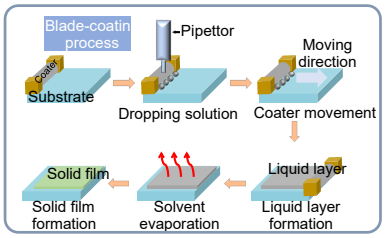

刘士浩，张乐天，谢文法*

吉林大学电子科学与工程学院 集成光电子学国家重点实验室
吉林大学实验区，吉林 长春 130012

摘要：有机电致发光器件 (OLED) 在照明领域的产业化发展仍然受到高成本的制约，而湿法 OLED 可显著降低制造成本。但是，相比于热蒸镀 OLED，湿法 OLED 在构建多层薄膜体系上面临更大的挑战。鉴于已有相关综述从材料工程角度对湿法 OLED 进行了总结，本文将主要从器件物理和制备工艺方面对湿法 OLED 进行概述。首先从器件载流子动力学和光物理角度分析各功能层的必要性。接着介绍常用的湿法薄膜制备工艺，并讨论制备多层湿法薄膜所涉及的问题。最后对湿法 OLED 的发展进行了展望。

关键词：湿法有机电致发光器件；多层结构；湿法制备工艺；电流平衡性；金属-电介质界面表面等离子体共振吸收

中图分类号：TN383.1　　**文献标志码：**A

刘士浩，张乐天，谢文法. 湿法有机电致发光器件：结构、器件物理及制备工艺 [J]. 光电工程，2022，**49**(5): 210407
Liu S H, Zhang L T, Xie W F. Solution processed organic light-emitting devices: structure, device physics and fabrication process[J]. *Opto-Electron Eng*, 2022, **49**(5): 210407

Solution processed organic light-emitting devices: structure, device physics and fabrication process

Liu Shihao, Zhang Letian, Xie Wenfa*

State Key Laboratory of Integrated Optoelectronics, College of Electronic Science and Engineering, Jilin University, Changchun, Jilin 130012, China

Abstract: The industrialization of organic light-emitting devices (OLEDs) in the field of lighting still faces the challenge of high costs, while solution-processed OLEDs can dramatically reduce their manufacturing cost. However, compared with thermally evaporated OLEDs, solution-processed OLEDs encounter difficulty in building multilayer systems. As the relevant reviews on solution-processed OLED from the perspective of material engineering have been proposed, this paper will mainly summarize multilayer structures of solution-processed OLED from the aspects of device physics and preparation processes. First, we will analyze the necessity of each functional layer based on the carrier/exciton dynamics and optical physics. Next, we will introduce the commonly used solution-processing techniques and discuss the problems involved in the preparation of multilayer films. Finally, we will present the future prospects of solution-processed OLEDs.

Keywords: solution-processed OLEDs; multilayer; solution-processing techniques; current balance; surface plasma resonance

收稿日期：2021-12-22；收到修改稿日期：2022-02-23
基金项目：国家自然科学基金资助项目 (61905086，62174067，62175085)；吉林省自然科学基金资助项目 (20190101024JH，20200201296JC)
*通信作者：谢文法，xiewf@jlu.edu.cn。

1 引 言

经过三十几年的发展，有机电致发光器件 (organic light-emitting devices, OLED) 已经从实验室器件发展成普通大众所熟知的智能手机屏幕。据市场分析估计，2021 年全球 OLED 显示面板市场规模约为 384 亿美元，预计到 2026 年将达到 728 亿美元。同样地，在照明领域，OLED 无论在装饰性照明还是功能性照明都拥有独特的优势。与 LED 点光源和荧光灯线光源相比，OLED 是一种面光源技术，发光与自然漫射光相近，柔和不刺眼，且具有轻、薄、可柔性等优势。然而，与显示领域相比，OLED 照明的产业化进展相对迟缓，这主要因为照明应用对成本更为敏感。根据美国能源部照明研发报告，LED 照明的每千流明成本可于 2025 年降到 0.45 美元，而 OLED 照明的每千流明成本将仍然保持在 30 美元左右[1]。

由于不依赖于高真空环境，湿法工艺无需复杂、昂贵的真空设备，为大幅降低 OLED 的制造成本提供了可能。但是，与真空热蒸镀器件相比，湿法 OLED 在器件结构上受到一定限制。经过 30 多年的发展，OLED 器件已从最开始的简单结构 (ITO/ N, N'-二苯基联苯胺 (N, N′-diphenylbenzidine, NPB)/三-(8-羟基喹啉) 铝(tris(8-hydroxyquinoline)aluminum，Alq_3)/LiF/Al) 发展为复杂的多层结构[2-10]。在传输层及发光层之外，载流子注入层和载流子/激子阻挡层也被引入以改善电流平衡性和提高激子利用率，因此 100% 内量子效率的 OLED 器件已被证实[11-20]。由于湿法工艺中溶剂会在一定程度上或完全溶解前一层预沉积的薄膜，湿法 OLED 在构建多层湿法薄膜体系上面临着挑战，因此湿法 OLED 在性能上通常相对逊色[21-25]。目前报道的大部分湿法 OLED 主要采用双层湿法薄膜体系，即采用聚合物传输层结合聚合物发光层或有机小分子混掺发光层，并仍需要热蒸镀必要的功能层来获得良好器件性能[26-28]。此外，一些特定的正交溶剂策略及交联型功能性材料也被提出并实现全湿法多层 OLED，包括全湿法叠层 OLED，为全湿法 OLED 提供了可能[29-31]。

鉴于已有相关综述很好地总结了湿法 OLED 所涉及的材料体系及正交溶剂策略[32-33]，本文将主要从器件物理和制备工艺方面概述湿法 OLED 的多层结构，并从器件物理角度分析各功能层的必要性，为湿法 OLED 的结构设计提供理论支撑。通过对典型的湿法薄膜制备工艺的介绍，将讨论现有工艺在构建多层湿法薄膜时所面临的问题。最后，对多层湿法 OLED 的发展方向也进行了一定展望。

2 湿法 OLED 结构

目前湿法 OLED 仍然广泛采用“三明治”器件结构，其主要原因有：1) 两侧平面电极之间距离在纳米尺度 (~100 nm) 时，低压 (<10 V) 可形成均匀的强电场 (10^7 V/m~10^8 V/m)，使非晶态半导体材料实现良好的载流子注入和传输。2) 采用多层结构可精准调控载流子/激子动力学行为，改善电流平衡性问题，提升激子辐射复合几率。由于 OLED 发光涉及空穴、电子两种类型载流子的动力学行为，为保证高发光效率，湿法 OLED 通常采用多层有机功能层才可以满足平衡的载流子注入/传输和高效的激子复合的需求。

2.1 器件结构

2.1.1 正置结构

正置结构，即阳极位于衬底而阴极位于器件顶部，是目前湿法 OLED 最常见的结构，这是因为在有机半导体表面继续沉积金属电极更易于实现低的电子注入势垒[34-35]。如图 1(a) 所示，湿法 OLED 的正置结构可分为两类，其中第一类包含空穴注入/传输层 (hole injection layer/hole transport layer，HJL/HTL) 及发光层 (emitting layer，EML)，第二类包含 HJL/HTL、EML 及电子传输/注入层 (electron transport layer/electron injection layer， ETL/EJL)。在第一类结构中，EML 可以同时起到电子注入/传输的功能。因此，该类结构比较简单，但限定了发光层材料的选择，通常为聚合物材料或混掺材料体系。发光单元可以通过化学聚合或物理混掺杂载流子传输单元，使发光层具备发光和载流子注入/传输的多功能性[36]。Burns 等采用具有电子传输特性的超黄色发光共聚物 (poly(1,4-phenylene-1,2-ethenediyl)，Super Yellow) 作为发光层，结合聚 (3,4-亚乙二氧基噻吩)-聚 (苯乙烯磺酸) (poly (3,4-ethylenedioxythiophene) polystyrene sulfonate, PEDOT:PSS) 作为空穴传输层，制备了最高电流效率 (current efficiency，CE) 为 12.0 cd/A 和最高外量子效率 (external quantum efficiency，EQE) 为 4.1% 的湿法 OLED[37]。Al-Attar 等采用空穴传输型的聚乙烯咔唑 (polyvinyl carbazole，PVK) 混掺杂电子传输型的 2-(4-叔丁苯基)-5-(4-联苯基)-1,3,4-恶二唑 (2-(4-tert-Butylphenyl)-5-(4-biphenylyl)-1,3,4-oxadiazole， PBD) 作为主体，结合磷光染料制备了最高 CE 为 40 cd•A^{-1}

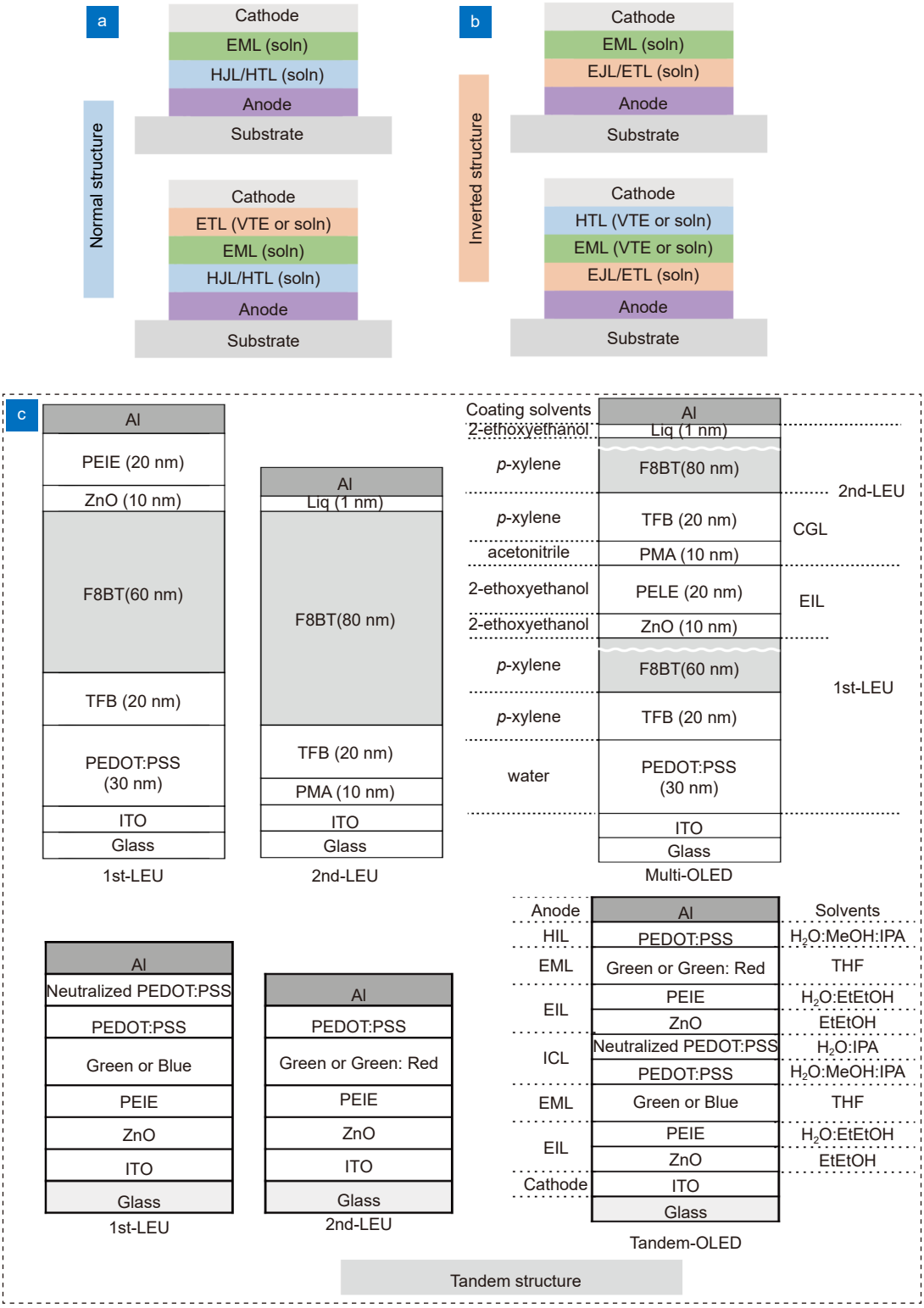

图 1　湿法 OLED 的器件结构示意图。

(a) 正置结构; (b) 倒置结构; (c) 叠层结构。

括号中所示 soln 代表湿法制备，而 VTE 代表热蒸镀制备[30−31]

Fig. 1　Schematic diagrams of device structures of solution-processed OLEDs.

(a) Normal structure; (b) Inverted structure; (c) Tandem structure. Soln and VTE in bracket respectively represent solution-processed and thermally evaporated under high vacuum[30−31]

和最高 EQE 为 12% 的单层湿法 OLED[38]。

为规避材料选择范围的限制，图 1(a) 所示第二类结构是目前湿法 OLED 更为普遍的结构。在该类结构中，独立的电子传输层被引入以促进电子注入及调控激子分布。与第一类结构相比，采用该类结构的湿法 OLED 通常在性能上具有明显的优势。Joseph Shinar 等在 4,4′-双 (N-咔唑)-1,1′-联苯 (4,4′-Di(9H-carbazol-9-yl)-1,1′-biphenyl, CBP): N,N′-二苯基-N,N′-二 (3-甲基苯基)-1,1′-联苯-4,4′-二胺 (N,N′-Diphenyl-N,N′-di(m-tolyl) benzidine, TPD):PBD: 三 [2-(对甲苯基) 吡啶-c2,n) 合铱 (III) (tris[2-(p-tolyl)pyridine]iridium(III), Ir(mppy)$_3$) 湿法发光层上继续蒸镀 4,7-二苯基-1,10-菲咯啉 (Bathophenanthroline, BPhen) 作为电子传输层制备了湿法磷光 OLED，该器件的最高 CE 和 EQE 分别达到 69 cd·A^{-1} 和 22% [39]。Hwang 等在湿法薄膜上继续蒸镀电子传输层 1,3,5-三 (1-苯基-1H-苯并咪唑-2-基) 苯 (2,2′,2″-(1,3,5-Benzinetriyl)-tris(1-phenyl-1-H-benzimidazole), TPBi)，实现了 EQE 为 17.5% 的湿法热活化延迟荧光 (thermally activated delayed fluorescence, TADF) OLED [40]。Pu 等采用正交溶剂体系在以共价二聚体和三聚体为主体的湿法发光层上继续旋涂 TPBi 电子传输层，实现了功率效率 (power efficiency, PE) 和 EQE 分别为 45 lm•W^{-1} 和 22% 的白光湿法 OLED [29]。由于有机分子具有相近的极性，第二类结构的电子传输层的湿法制备方式受到了一定限制，需要采用特定的正交溶剂体系或交联型发光层才能在发光层上湿法制备电子传输层。因此，目前大部分第二类结构的湿法 OLED 依然采用热蒸镀工艺制备电子传输层。

2.1.2 倒置结构

倒置结构，也是湿法 OLED 所常用的器件结构。如图 1(b) 所示，倒置结构中阴极位于衬底而阳极位于器件顶部。由于阴极位于底部，倒置结构可采用迁移率较高的金属氧化物作为电子传输层，有助于弥补有机半导体在电子迁移率上的短板，进而改善器件的工作电流范围及载流子平衡性。此外，由于惰性金属电极可实现空穴的欧姆注入，倒置结构无需采用活泼金属作为顶部电极，被认为是实现高稳定性的理想器件结构[41]。与正置结构相同，倒置结构也可以采用具有多功能性的聚合物或掺杂型发光层。Lee Tae-Woo 等采用 Super Yellow 做发光层，结合 ZnO/乙氧基化的聚乙烯亚胺 (ethoxylated polyethyleneimine，PEIE) 电子传输层及 MoO_3 修饰的银阳极，制备了最高 CE 为 13.8 cd•A^{-1} 的湿法倒置 OLED[42]。马东阁等采用 2,7-双 (二苯基氧膦基)-9,9′-螺双 [芴] (2,7-Bis(diphenylphosphoryl)-9,9′-spirobifluorene, SPPO13) 和三 (4-咔唑基-9-基苯基) 胺 (tris(4-carbazoyl-9-ylphenyl)amine, TCTA) 混掺主体，结合蒸镀 TCTA 空穴传输层制备了湿法倒置 OLED，其最高 CE 和 EQE 分别为 56.9 cd•A^{-1} 和 16.3%[43]。然而，目前报道的大部分倒置器件仅电子传输层采用湿法工艺制备，而其它功能层仍然依赖于热蒸镀工艺[20,44-45]。例如，我们课题组在旋涂工艺制备氧化钛 (Titanium dioxide，TiO_2) 的基础上，依次蒸镀三层电子界面修饰层、发光层、空穴传输层和金属阳极，实现了 EQE 达到 18% 的倒置 OLED，这是目前报道的基于 TiO_2 的器件最高记录[45]。

2.1.3 叠层结构

叠层结构，即通过由电子给体材料和电子受体材料组成的电荷生成层将多个发光单元相互连接所形成的结构，可以利用更少的电流产生更高的亮度，有助于降低效率滚降并改善工作寿命，对于推动 OLED 照明应用具有重要意义。叠层器件的阴阳极之间通常具有十数层以上的功能层，这导致湿法叠层器件的制备面临更大的挑战。目前报道的湿法叠层器件相对较少，图 1(c) 所示为目前最具代表性的两个湿法叠层 OLED[30-31]。其中在正置叠层结构 (图 1(c)) 中，Pu 等依次采用水、对二甲苯、对二甲苯、二乙氧基乙醇、二乙氧基乙醇、乙腈、对二甲苯、对二甲苯、二乙氧基乙醇，通过旋涂工艺制备了 PEDOT:PSS\聚 (9, 9-二辛基芴-CO-N-(4-丁基苯基) 二苯胺) (poly(9,9-dioctylfluorene-alt-N-(4-sec-butylphenyl)-diphenylamine), TFB)\聚 (9,9-二辛基芴基-2,7-二基) (Poly(9,9-dioctylfluorene-alt-benzothiadiazole), F8BT)\ZnO\PEIE\钼磷酸 (phosphomolybdic acid hydrate, PMA)\TFB\F8BT\8-羟基喹啉-锂 (8-Hydroxyquinolinolato-lithium, Liq) 共 9 层有机功能层。这两个器件所采用的正交溶剂体系及材料体系对后续湿法叠层器件的制备产生了重要的启示作用[46-47]。

2.2 电流平衡性

多层结构对于器件高效率的必要性，在很大程度上与 OLED 的电流平衡性有关。OLED 的载流子动力学涉及两种类型的载流子，即空穴与电子。由于电荷守恒和电流连续性，器件具有统一的复合电流 I_R。然而，由于器件两侧 (一侧为阳极至发光层，另一侧为阴极至发光层) 的界面势垒及传输特性并不完全一致，

因此在相同电场下，阴阳电极注入的电子电流 I_e 和空穴电流 I_h 并不一致。根据 Marburg 模型[48-51]，一个工作状态的 OLED 的电流存在以下关系：

$$I_h = I_R + I_{h'} + \frac{dQ_h}{dt}, \tag{1}$$

$$I_e = I_R + I_{e'} + \frac{dQ_e}{dt}, \tag{2}$$

$$I_{ext} = I_h + \frac{dQ_A}{dt} + I_{e'} = I_e + \frac{dQ_c}{dt} + I_{h'}, \tag{3}$$

其中：I_{ext} 为外部电流，$I_{h'}$和 $I_{e'}$分别为越过复合区的空穴漏电流和电子漏电流。Q_A 及 Q_h 分别为阳极界面和器件内部积累的空穴载流子，Q_C 及 Q_e 则分别为阴极界面和器件内部积累的电子载流子。根据式 (1) 和式 (2)，可以获得复合电流 I_R 的表达式：

$$I_R = I_h - I_{h'} - \frac{dQ_h}{dt} = I_e - I_{e'} - \frac{dQ_e}{dt}. \tag{4}$$

根据该模型，可以看出器件的电流平衡性可以通过两种方式实现，即多子电流的漏电流及内部载流子积累。以空穴主导的 OLED 为例 (如图 2)，电子漏电

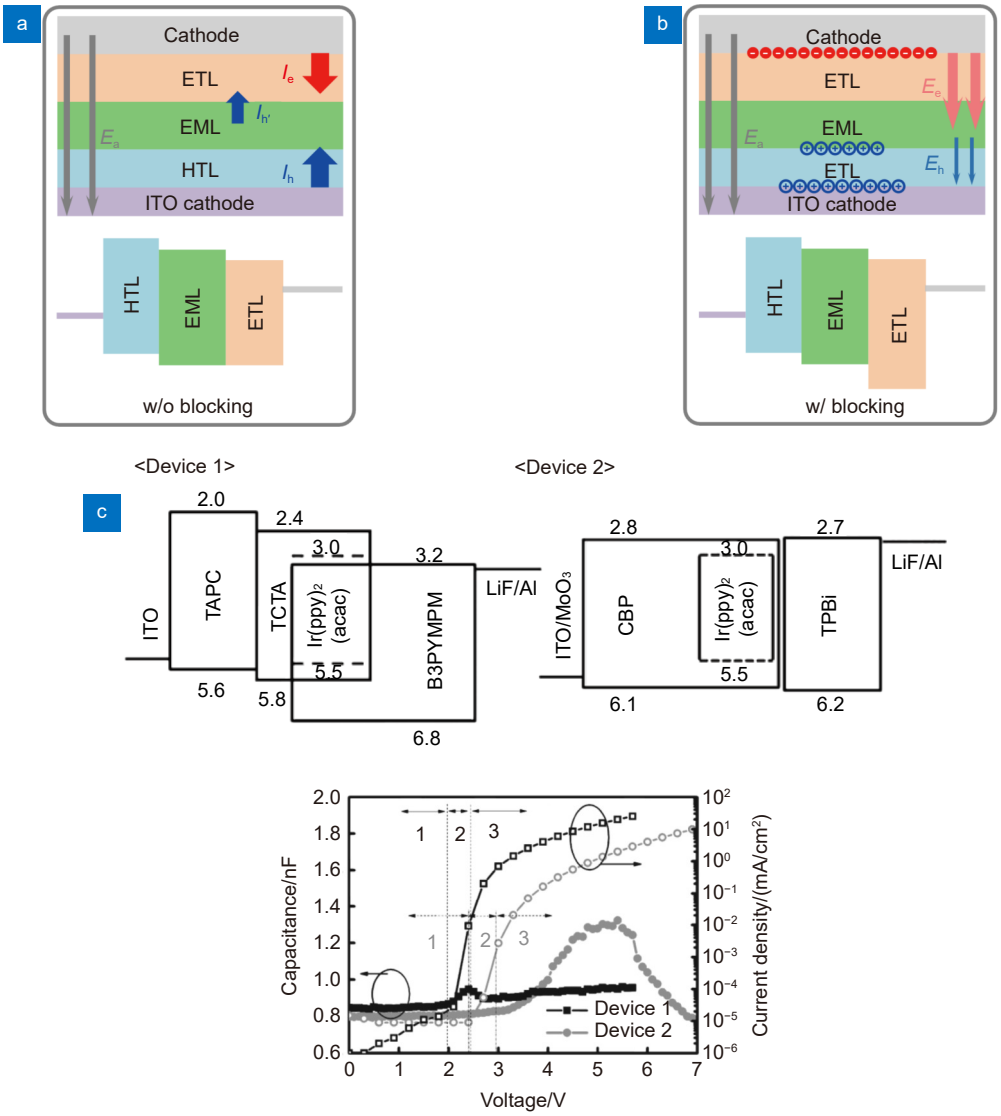

图 2　空穴主导型 OLED 器件的电流平衡性示意图。

(a) ETL 不具有空穴阻挡作用的情况；(b) ETL 具有空穴阻挡作用的情况；

(c) 空穴主导型 OLED 器件的能级图及电容-电压-电流密度特性[52]

Fig. 2　Schematic diagrams of current balance in hole-dominated OLEDs.

(a) A case of ETL without hole blocking; (b) A case of ETL with hole blocking;

(c) Energy levels and capacitance-voltage-current density characteristics of two hole-dominated OLEDs[52]

流 I_e 和电子载流子积累 dQ_e/dt 可被忽略，式 (4) 可以被简化为

$$I_R = I_h - I_{h'} - \frac{dQ_h}{dt} = I_e \,. \tag{5}$$

如图 2(a) 所示，在空穴主导型 OLED中，当 ETL 无法阻挡空穴载流子的情况下，空穴漏电流 I_h对于电流平衡起主导作用[52]。然而，漏电流的存在将导致器件性能及寿命受到严重制约。目前报道的 OLED 器件通常引入具有适当能级或迁移率的载流子阻挡层，将载流子限制于 EML 中，因此在这种情况下，多数载流子积累 dQ_h/dt 对于电流平衡性起主导作用[52]。如图 2(b) 所示，内部空穴载流子的积累 dQ_h/dt 将改变内部电场强度分布，增强电子传输电流及减弱空穴传输电流，使二者达到动态平衡。需要注意的是，在这种情况下，由于 EML/ETL 界面积累的载流子将产生严重的极化子-激子猝灭。EML 为空穴主导型或双极型时，激子复合区与载流子积累区有一定重合，器件性能将受到严重影响。在热蒸镀器件中，额外的功能层，如载流子阻挡层，常被引入分离载流子积累区和激子复合区。例如，在许多报道器件中 4,4′-环己基二 [N,N-二 (4-甲基苯基) 苯胺] (4,4′-Cyclohexylidenebis [N,N-bis(4-methylphenyl)benzenamine], TAPC)/TCTA 双层结构常被用做 HTL[52-55]。如图 2(c) 所示，Kim 等人研究表明在采用 4,4 ′-双 (N - 咔唑)-1,1′-联苯 (4,4 - N , N ′- Dicarbazole -1,1′- biphenyl, CBP) 单层 HTL 的器件中，载流子积累主要集中在发光染料上；而引入 TAPC/TCTA 双层 HTL 后，载流子可以在 TAPC/TCTA 界面积累，进而改善了器件性能 [52]。然而，在湿法 OLED 中，层数的增加受到工艺的严重制约，限制了器件性能的提升。

2.3 表面等离子体激元 (SPP) 共振吸收

金属-电介质界面存在一种相干的离域电子振荡 (如图 3(a) 所示)，即表面等离子体 (surface plasmons,

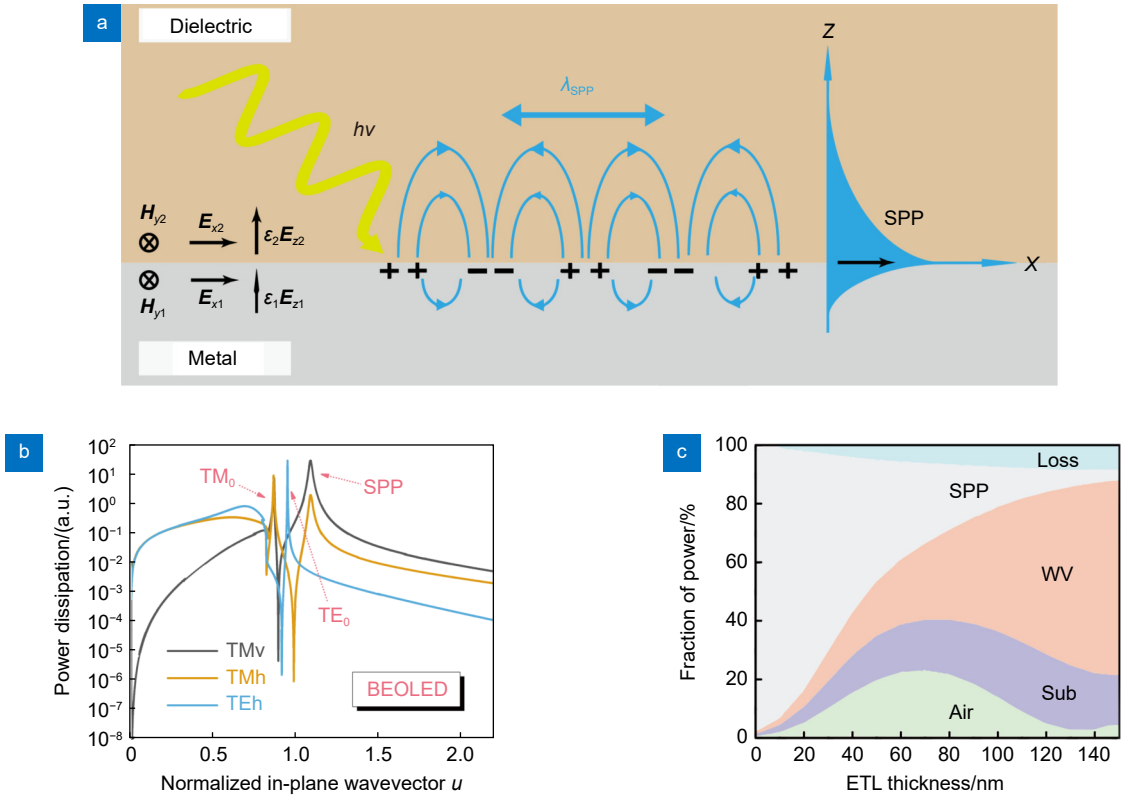

图 3 (a) 电介质-金属界面的表面等离子体激元示意图; (b) OLED 中偶极子辐射的功率耗散谱, TMv、TMh 及 TEh 分别对应于纵向偶极子的 TM 模，水平偶极子的 TM 模和 TE 模[14]; (c) 不同 ETL 厚度 OLED 的光功率模态分析。Air、Sub、WV、SPP 和 Loss 分别对应于空气模、衬底模、波导模、SPP 模和金属吸收模[56]

Fig. 3 (a) Schematic diagram of SPP at metal-dielectric surface; (b) Power dissipation spectra of dipole radiation. TMv, TMh and TEh respectively represent TM mode from vertical dipole, TM mode and TE mode from horizontal dipole[14]; (c) Optical power modal analysis vs ETL thickness of a conventional OLED. The power is distributed into air (Air), substrate (Sub), waveguide (WV), surface plasmon polariton (SPP) and lossy metal (Loss) modes[56]

SPs)。通常情况下，具有相同频率和动量的光子与SPs才能发生耦合，形成表面等离子体激元 (surface plasmon polariton，SPP)。在给定频率下，由于自由空间的光子的动量通常小于SPP，因此自由空间的光子无法直接激发SPP。然而，在OLED中，电极与发光层的距离通常远小于可见光波长，因此金属/有机界面位于偶极子光源的近场位置。如图 3(b) 所示，由于近场复杂的电磁特征，发光层产生的光子可以激发有机介质/金属电极界面的SPP[14]。然而，由于波矢量不匹配，金属/有机界面的SPP将无法再以光子的形式将能量传递出 (仅适用常规OLED中均匀的金属/有机界面)。因此，SPP共振将会吸收一部分OLED的光功率，是造成光损耗的重要原因之一 (如图 3(c))。由于SPP共振与近场特性有关，增加ETL厚度 (即激子复合区与金属电极距离) 可以有效地降低SPP模损耗[56]。如图 3(c) 所示，在ETL厚度为60 nm时，器件光取出效率 (Air模) 最高。这表明为获得高性能，激子复合区应与金属电极之间保持一定的距离。多层结构在限定激子复合区位置具有显著的优势，如引入载流子/激子阻挡层及载流子传输层。因此，从光学角度看，多层结构对于高效率湿法OLED也是必要性条件。

3 湿法工艺

3.1 旋涂工艺

旋涂工艺是一种利用离心力将均匀薄膜沉积到基板上的工艺。通过轴对称中心旋转产生的离心力，牛顿流体材料可以均匀散步在基材表面，待挥发性溶剂蒸发后获得具有纳米级厚度的均匀薄膜[57]。如图 4(a) 所示，旋涂工艺主要包含四个过程：点胶、自旋加速、匀胶及挥发成膜。通过控制所涉及的几个工艺参数，如匀胶时间、转速、溶液浓度、粘度，成膜厚度可以得到精确控制。由于离心力作用下的自流平，旋涂薄膜在膜厚均匀性上具有很大优势，厚度变化通常不超过1%。因此，旋涂工艺被广泛地应用于半导体器件的制备[20,45,58-60]。然而，旋涂工艺制备多层有机薄膜面临诸多物理限制，而且只适用于在平面状简单工件上制备单侧涂层。在旋涂制备多层薄膜时，下层薄膜在点胶到挥发成膜整个过程持续承受溶剂的溶解或溶胀。因此，一般情况下，旋涂工艺需要结合合适的正交溶剂体系或交联型材料制备多层湿法薄膜[29-31]。多数报道的正交溶剂体系是基于高分子量聚合物。Pu等证实当分子量高于某临界值时，小分子也可以承受基于正交溶剂体系的多层湿法工艺[29]。但是，大多数EML溶于非极性有机溶剂，因此后续湿法薄膜的制备通常需要依赖极性较高的醇或水等溶剂。然而，强极性的传输层材料在一定程度上将产生内部载流子积累问题，严重影响器件的发光效率[61]。

3.2 喷涂工艺

喷涂工艺是以喷射液滴或粒子的形式将材料沉积在基板上的涂膜工艺，如图 4(b) 所示。湿法OLED制备所涉及的喷涂工艺主要采用溶液雾化的方式，首先通过喷嘴将溶液雾化成微米级液滴，然后在气流驱动或自身惯性下，将这些液滴广泛地分布在基板上，并在表面张力作用下合并成连续的液膜，待溶剂蒸发后形成固态膜。借助于掩模版，喷涂工艺可以湿法制备图案化薄膜[62]。然而，在溶剂蒸发阶段，与旋涂工艺不同的是，喷涂工艺不存在离心力移除多余的溶液，溶液厚度通常远超过衬底表面作用力或静电力的作用范围。因此，复杂的流体运动，如毛细流动及Marangoni流动等，往往导致固态膜的均匀性存在严重的问题。为了改善喷涂薄膜的均匀性，Girotto等人利用双溶剂体系建立表面张力梯度以增强马兰戈尼流动，成功实现了高品质的喷涂PEDOT:PSS薄膜及聚合物有源层[63]。我们通过引入辅助溶剂在液膜边缘建立稳定的张力平衡体系防止液膜收缩，减缓了咖啡环效应，制备出均匀的有机小分子薄膜，器件的最高发光效率为24.7 cd/A，与具有相同器件结构的真空蒸镀器件性能相当[64]。此外，我们还采用斜坡超声喷涂工艺改善大面积薄膜均匀性，利用重力有效地限制液膜中复杂流动行为，制备出了高质量的多组分发光薄膜，获得的双色白光器件的最高电流、功率及外量子效率达到29.5 cd/A、28.1 lm/W及14.1%，与真空蒸镀器件性能相当[65]。

3.3 刮涂工艺

刮涂工艺是通过在平台表面移动刮刀，使流体通过狭窄间隙形成均匀液膜，待溶剂挥发后形成固态薄膜的工艺。通过调控衬底温度及刮刀移动速度，刮涂工艺可以精确控制溶剂挥发速率，减少底层薄膜对溶剂的耐受时间，在实现多层湿法薄膜方面具有重要优势。我国台湾地区Yeh等人通过控制80°C基板温度结合热风流动，加快溶剂挥发速度，采用刮涂法制备了均匀的多层结构，所实现的蓝光全湿法器件的最高EQE为10.8%，白光全湿法器件的最高EQE为11.6%[66]。当采用Landau-Levich模式刮涂时，液膜形

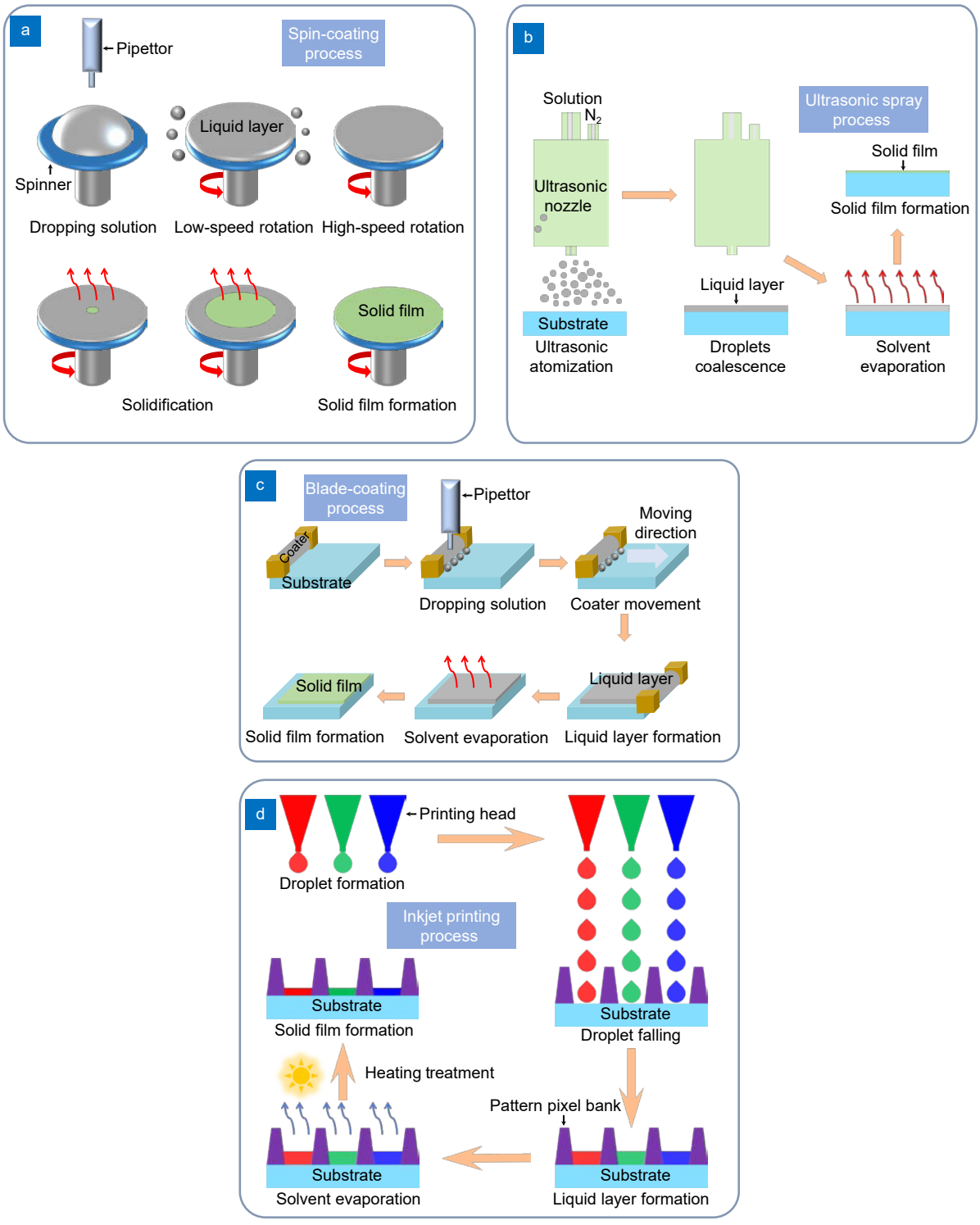

图 4　湿法工艺示意图。

(a) 旋涂工艺; (b) 超声喷涂工艺[64]; (c) 刮涂工艺; (d) 喷墨打印工艺

Fig. 4　Schematic diagram of solution-processing technologies.

(a) Spin coating process; (b) Ultrasonic spray coating process[64]; (c) Blade coating process; (d) Inkjet printing process

成后存在的流体运动将难以被忽略，所制备固态膜的均匀性存在一定问题。为了改善成膜均匀性，表面活性剂或双溶剂体系被相继提出[67-68]。此外，结合表面能处理技术或图案化丝网，刮涂工艺也可以完成图案化薄膜制备[9,69]。

3.4 喷墨打印

喷墨打印是一种通过热发泡或陶瓷压电方式将墨滴喷射到基材上制备点、线、面型膜层的工艺。由于墨滴微粒形状规则、定位准确，喷墨打印技术可以借助电脑控制实现高精度图案化膜层，在图案化薄膜制备方面具有显著优势[70-71]。通过控制墨滴液量或数目，喷墨打印工艺也可以不借助正交溶剂体系及交联型材料，制备多层有机小分子膜[72]。此外，咖啡环效应也影响喷墨打印薄膜的成膜质量。双溶剂体系也被提出用来改善喷墨打印薄膜的均匀性[73]。但是，储墨腔壁的存在改变了液膜的张力平衡体系，在一定程度上减弱了咖啡环效应的影响，将影响限制在边缘区域[74-75]。

4 结论与展望

4.1 结论

本文综述了湿法有机发光器件的多层结构，包括正置结构、倒置结构及叠层结构。从器件物理角度，分析了多层器件结构有助于改善器件电流平衡性，降低内部载流子积累或漏电流对器件效率和寿命的影响，并且讨论了多层结构有利于降低金属-电介质界面 SPP 共振吸收，对实现高性能湿法器件具有重要作用。

同时还讨论了四种典型的湿法薄膜制备工艺：旋涂、喷涂、刮涂及喷墨打印在构建多层湿法薄膜时所面临的问题。由于离心力作用下的自流平，旋涂薄膜在成膜均匀性上具有优势。正交溶剂体系及交联型材料策略可以实现多层旋涂薄膜，但可能导致器件面临载流子陷阱、积累等问题。由于毛细流动及 Marangoni 流动的影响，喷涂、刮涂及喷墨打印的成膜需要借助表面活性剂或双溶剂体系。此外，刮涂和喷墨打印可以精确控制液膜量及其干燥速率，能够不借助正交溶剂体系及交联型材料策略实现多层湿法薄膜的制备，但受到设备精度及溶剂特性的限制。

4.2 展望

综上所述，多层结构是实现高性能湿法 OLED 的必要性条件，且现有工艺体系制备多层湿法薄膜具有可行性。但由于有机分子极性相似，现有湿法工艺在普适性方面仍存在问题。现有湿法工艺低成本的优势在于不依赖高真空，而存在问题主要由于溶剂的使用所导致。在钙钛矿领域，韩立元教授团队研发出一种无溶剂、非真空的新沉积方案用于甲基铵卤化铅钙钛矿薄膜的制备，即软膜压印法[76]。该工艺既可以保留湿法工艺的低成本优势，又可以避免引入溶剂所产生的问题，在构建低成本多层 OLED 方面具有巨大潜力。

参考文献

[1] Pattison M, Hansen M, Bardsley N, et al. 2019 lighting R&D opportunities[R]. Santa Barbara: Solid State Lighting Solutions (SSLS) Inc. , 2020. doi: 10.2172/1618035.

[2] Tang C W, VanSlyke S A. Organic electroluminescent diodes[J]. *Appl Phys Lett*, 1987, **51**(12): 913−915.

[3] Liao L S, Klubek K P, Tang C W. High-efficiency tandem organic light-emitting diodes[J]. *Appl Phys Lett*, 2004, **84**(2): 167−169.

[4] Uoyama H, Goushi K, Shizu K, et al. Highly efficient organic light-emitting diodes from delayed fluorescence[J]. *Nature*, 2012, **492**(7428): 234−238.

[5] Gather M C, Köhnen A, Meerholz K. White organic light-emitting diodes[J]. *Adv Mater*, 2011, **23**(2): 233−248.

[6] Wen X M, Bi Y G, Yi F S, et al. Tunable surface plasmon-polariton resonance in organic light-emitting devices based on corrugated alloy electrodes[J]. *Opto-Electron Adv*, 2021, **4**(8): 200024.

[7] Liu S H, Liu W B, Yu J, et al. Silver/germanium/silver: an effective transparent electrode for flexible organic light-emitting devices[J]. *J Mater Chem C*, 2014, **2**(5): 835−840.

[8] Li Z T, Cao K, Li J S, et al. Review of blue perovskite light emitting diodes with optimization strategies for perovskite film and device structure[J]. *Opto-Electron Adv*, 2021, **4**(2): 200019.

[9] Wang Y, Liu S H, Dang F Y, et al. An efficient flexible white organic light-emitting device with a screen-printed conducting polymer anode[J]. *J Phys D Appl Phys*, 2012, **45**(40): 402002.

[10] Zhang X, Liu S H, Zhang L T, et al. In-planar-electrodes organic light-emitting devices for smart lighting applications[J]. *Adv Opt Mater*, 2019, **7**(3): 1800857.

[11] Liu S H, Zhang X, Wang S R, et al. Hybrid organic light-emitting device based on ultrasonic spray-coating molybdenum trioxide transport layer with low turn-on voltage, improved efficiency & stability[J]. *Org Electron*, 2018, **52**: 264−271.

[12] Liu S H, Zhang X, Feng H W, et al. Two-dimensional-growth small molecular hole-transporting layer by ultrasonic spray coating for organic light-emitting devices[J]. *Org Electron*, 2017, **47**: 181−188.

[13] Liu W B, Liu S H, Zhang W, et al. Angle-stable inverted top-emitting white organic light-emitting devices based on gradient-doping electron injection interlayer[J]. *Org Electron*, 2015, **25**: 335−339.

[14] Zang C X, Liu S H, Xu M X, et al. Top-emitting thermally

activated delayed fluorescence organic light-emitting devices with weak light-matter coupling[J]. *Light Sci Appl*, 2021, **10**(1): 116.

[15] Zhang X, Pan T, Zhang J X, et al. Color-tunable, spectra-stable flexible white top-emitting organic light-emitting devices based on alternating current driven and dual-microcavity technology[J]. *ACS Photonics*, 2019, **6**(9): 2350−2357.

[16] Yin M J, Pan T, Yu Z W, et al. Color-stable WRGB emission from blue OLEDs with quantum dots-based patterned down-conversion layer[J]. *Org Electron*, 2018, **62**: 407−411.

[17] Liu S H, Wen X M, Liu W B, et al. Angle-stable top-emitting white organic light-emitting devices employing a down-conversion layer[J]. *Curr Appl Phys*, 2014, **14**(11): 1451−1454.

[18] Yu Z W, Feng H W, Zhang J X, et al. Carrier transport manipulation for efficiency enhancement in blue phosphorescent organic light-emitting devices with a 4, 4′-bis (*N*-carbazolyl)-2, 2′-biphenyl host[J]. *J Mater Chem C*, 2019, **7**(30): 9301−9307.

[19] Zhang X, Liu S H, Zhang Y Q, et al. Efficiently alternating current driven tandem organic light-emitting devices with (Ag/4, 7-diphenyl-1, 10-phenanthroline)$_n$ interconnecting layers[J]. *Appl Phys Lett*, 2017, **111**(10): 103301.

[20] Zang C X, Xu M X, Zhang L T, et al. Organic-inorganic hybrid thin film light-emitting devices: interfacial engineering and device physics[J]. *J Mater Chem C*, 2021, **9**(5): 1484−1519.

[21] Peng J H, Xu X J, Feng X J, et al. Fabrication of solution-processed pure blue fluorescent OLED using exciplex host[J]. *J Lumin*, 2018, **198**: 19−23.

[22] He Z Y, Wang C Y, Zhao J W, et al. Blue and white solution-processed TADF-OLEDs with over 20% EQE, low driving voltages and moderate efficiency decrease based on interfacial exciplex hosts[J]. *J Mater Chem C*, 2019, **7**(38): 11806−11812.

[23] Park S Y, Choi S, Park G E, et al. Unconventional three-armed luminogens exhibiting both aggregation-induced emission and thermally activated delayed fluorescence resulting in high-performing solution-processed organic light-emitting diodes[J]. *ACS Appl Mater Interfaces*, 2018, **10**(17): 14966−14977.

[24] Tang C, Yang T, Cao X D, et al. Tuning a weak emissive blue host to highly efficient green dopant by a CN in tetracarbazolepyridines for solution-processed thermally activated delayed fluorescence devices[J]. *Adv Opt Mater*, 2015, **3**(6): 786−790.

[25] Kim Y H, Wolf C, Cho H, et al. Highly efficient, simplified, solution-processed thermally activated delayed-fluorescence organic light-emitting diodes[J]. *Adv Mater*, 2016, **28**(4): 734−741.

[26] Li B, Yang Z, Gong W Q, et al. Intramolecular through-space charge transfer based TADF-active multifunctional emitters for high efficiency solution-processed OLED[J]. *Adv Opt Mater*, 2021, **9**(15): 2100180.

[27] Sun K Y, Liu D, Tian W W, et al. Manipulation of the sterically hindering effect to realize AIE and TADF for high-performing nondoped solution-processed OLEDs with extremely low efficiency roll-off[J]. *J Mater Chem C*, 2020, **8**(34): 11850−11859.

[28] Usta H, Alimli D, Ozdemir R, et al. A hybridized local and charge transfer excited state for solution-processed non-doped green electroluminescence based on oligo (*p*-phenyleneethynylene) [J]. *J Mater Chem C*, 2020, **8**(24): 8047−8060.

[29] Aizawa N, Pu Y J, Watanabe M, et al. Solution-processed multilayer small-molecule light-emitting devices with high-efficiency white-light emission[J]. *Nat Commun*, 2014, **5**(1): 5756.

[30] Pu Y J, Chiba T, Ideta K, et al. Fabrication of organic light-emitting devices comprising stacked light-emitting units by solution-based processes[J]. *Adv Mater*, 2015, **27**(8): 1327−1332.

[31] Chiba T, Pu Y J, Kido J. Solution-processed white phosphorescent tandem organic light-emitting devices[J]. *Adv Mater*, 2015, **27**(32): 4681−4687.

[32] Ho S, Liu S Y, Chen Y, et al. Review of recent progress in multilayer solution-processed organic light-emitting diodes[J]. *J Photonics Energy*, 2015, **5**(1): 057611.

[33] Zhong C M, Duan C H, Huang F, et al. Materials and devices toward fully solution processable organic light-emitting diodes[J]. *Chem Mater*, 2011, **23**(3): 326−340.

[34] Li Y, Zhang D Q, Duan L, et al. Elucidation of the electron injection mechanism of evaporated cesium carbonate cathode interlayer for organic light-emitting diodes[J]. *Appl Phys Lett*, 2007, **90**(1): 012119.

[35] Liu W B, Liu S H, Yu J, et al. Efficient inverted organic light-emitting devices with self or intentionally Ag-doped interlayer modified cathode[J]. *Appl Phys Lett*, 2014, **104**(9): 093305.

[36] Tokito S, Suzuki M, Sato F, et al. High-efficiency phosphorescent polymer light-emitting devices[J]. *Org Electron*, 2003, **4**(2-3): 105−111.

[37] Burns S, MacLeod J, Do T T, et al. Effect of thermal annealing Super Yellow emissive layer on efficiency of OLEDs[J]. *Sci Rep*, 2017, **7**(1): 40805.

[38] Al-Attar H A, Griffiths G C, Moore T N, et al. Highly efficient, solution-processed, single-layer, electrophosphorescent diodes and the effect of molecular dipole moment[J]. *Adv Funct Mater*, 2011, **21**(12): 2376−2382.

[39] Cai M, Xiao T, Hellerich E, et al. High-efficiency solution-processed small molecule electrophosphorescent organic light-emitting diodes[J]. *Adv Mater*, 2011, **23**(31): 3590−3596.

[40] Hwang J, Lee C, Jeong J E, et al. Rational design of carbazole- and carboline-based polymeric host materials for realizing high-efficiency solution-processed thermally activated delayed fluorescence organic light-emitting diode[J]. *ACS Appl Mater Interfaces*, 2020, **12**(7): 8485−8494.

[41] Fukagawa H, Sasaki T, Tsuzuki T, et al. Long-lived flexible displays employing efficient and stable inverted organic light-emitting diodes[J]. *Adv Mater*, 2018, **30**(28): 1706768.

[42] Kwon S J, Han T H, Kim Y H, et al. Solution-processed n-type graphene doping for cathode in inverted polymer light-emitting diodes[J]. *ACS Appl Mater Interfaces*, 2018, **10**(5): 4874−4881.

[43] Chen J S, Shi C S, Fu Q, et al. Solution-processable small molecules as efficient universal bipolar host for blue, green and red phosphorescent inverted OLEDs[J]. *J Mater Chem*, 2012, **22**(11): 5164−5170.

[44] Zhang J X, Zhang X, Feng H W, et al. An efficient and stable hybrid organic light-emitting device based on an inorganic metal oxide hole transport layer and an electron transport layer [J]. *J Mater Chem C*, 2019, **7**(7): 1991−1998.

[45] Zang C X, Wang H, Liu S H, et al. Efficiency enhancement in an inverted organic light-emitting device with a TiO_2 electron injection layer through interfacial engineering[J]. *J Mater Chem C*, 2020, **8**(24): 8206−8212.

[46] Ohisa S, Takahashi T, Igarashi M, et al. An indolocarbazole-based thermally activated delayed fluorescence host for solution-processed phosphorescent tandem organic light-emitting devices exhibiting extremely small efficiency roll-off[J]. *Adv Funct Mater*, 2019, **29**(16): 1808022.

[47] Höfle S, Bernhard C, Bruns M, et al. Charge generation layers for solution processed tandem organic light emitting diodes with regular device architecture[J]. *ACS Appl Mater Interfaces*, 2015, **7**(15): 8132−8137.

[48] Khramtchenkov D V, Bässler H, Arkhipov V I. A model of electroluminescence in organic double-layer light-emitting diodes[J]. *J Appl Phys*, 1996, **79**(12): 9283−9290.

[49] Nikitenko V R, Arkhipov V I, Tak Y H, et al. The overshoot effect in transient electroluminescence from organic bilayer light emitting diodes: Experiment and theory[J]. *J Appl Phys*, 1997, **81**(11): 7514−7525.

[50] Hassine L, Bouchriha H, Roussel J, et al. Transient response of a bilayer organic electroluminescent diode: experimental and theoretical study of electroluminescence onset[J]. *Appl Phys Lett*, 2001, **78**(8): 1053−1055.

[51] Hassine L, Bouchriha H, Roussel J, et al. Transient response of a bilayer organic light emitting diode: Building-up of external and recombination currents[J]. *J Appl Phys*, 2002, **91**(8): 5170−5175.

[52] Lee J H, Lee S, Yoo S J, et al. Langevin and trap-assisted recombination in phosphorescent organic light emitting diodes[J]. *Adv Funct Mater*, 2014, **24**(29): 4681−4688.

[53] Wang B Q, Kou Z Q, Tang Y, et al. High CRI and stable spectra white organic light-emitting diodes with double doped blue emission layers and multiple ultrathin phosphorescent emission layers by adjusting the thickness of spacer layer[J]. *Org Electron*, 2019, **70**: 149−154.

[54] Park Y S, Lee S, Kim K H, et al. Exciplex-forming co-host for organic light-emitting diodes with ultimate efficiency[J]. *Adv Funct Mater*, 2013, **23**(39): 4914−4920.

[55] Xu H W, Lin J Y, Jiang X X, et al. Study on the difference in exciton generation processes for a single host and exciplex-type co-host[J]. *Opt Lett*, 2021, **46**(19): 4840−4843.

[56] Qu Y, Kim J, Coburn C, et al. Efficient, nonintrusive outcoupling in organic light emitting devices using embedded microlens arrays[J]. *ACS Photonics*, 2018, **5**(6): 2453−2458.

[57] Sahu N, Parija B, Panigrahi S. Fundamental understanding and modeling of spin coating process: a review[J]. *Indian J Phys*, 2009, **83**(4): 493−502.

[58] Liu S H, Wang Y C, Chang C M, et al. Solution-processed organometallic quasi-two-dimensional nanosheets as a hole buffer layer for organic light-emitting devices[J]. *Nanoscale*, 2020, **12**(13): 6983−6990.

[59] Guan Z Q, Li Y, Zhu Z H, et al. Efficient perovskite white light-emitting diode based on an interfacial charge-confinement structure[J]. *ACS Appl Mater Interfaces*, 2021, **13**(37): 44991−45000.

[60] Feng H W, Liu S H, Tang G, et al. Highly efficient and stable quantum dot light-emitting devices with a low-temperature tin oxide electron transport layer[J]. *J Mater Chem C*, 2021, **9**(39): 13748−13754.

[61] Bangsund J S, Van Sambeek J R, Concannon N M, et al. Sub-turn-on exciton quenching due to molecular orientation and polarization in organic light-emitting devices[J]. *Sci Adv*, 2020, **6**(32): eabb2659.

[62] Liu S H, Yu H W, Zhang Q Y, et al. Efficient ITO-free organic light-emitting devices with dual-functional PSS-rich PEDOT: PSS electrode by enhancing carrier balance[J]. *J Mater Chem C*, 2019, **7**(18): 5426−5432.

[63] Girotto C, Moia D, Rand B P, et al. High-performance organic solar cells with spray-coated hole-transport and active layers[J]. *Adv Funct Mater*, 2011, **21**(1): 64−72.

[64] Liu S H, Zhang X, Zhang L T, et al. Ultrasonic spray coating polymer and small molecular organic film for organic light-emitting devices[J]. *Sci Rep*, 2016, **6**(1): 37042.

[65] Liu S H, Zhang X, Yin M J, et al. Coffee-ring-free ultrasonic spray coating single-emission layers for white organic light-emitting devices and their energy-transfer mechanism[J]. *ACS Appl Energy Mater*, 2018, **1**(1): 103−112.

[66] Yeh H C, Meng H F, Lin H W, et al. All-small-molecule efficient white organic light-emitting diodes by multi-layer blade coating[J]. *Org Electron*, 2012, **13**(5): 914−918.

[67] Deng Y H, Zheng X P, Bai Y, et al. Surfactant-controlled ink drying enables high-speed deposition of perovskite films for efficient photovoltaic modules[J]. *Nat Energy*, 2018, **3**(7): 560−566.

[68] Yu H W, Zhang J M, Long T, et al. Efficient all-blade-coated quantum dot light-emitting diodes through solvent engineering[J]. *J Phys Chem Lett*, 2020, **11**(21): 9019−9025.

[69] Han D, Khan Y, Ting J, et al. Flexible blade-coated multicolor polymer light-emitting diodes for optoelectronic sensors[J]. *Adv Mater*, 2017, **29**(22): 1606206.

[70] Amruth C, Szymański M Z, Łuszczyńska B, et al. Inkjet printing of super yellow: ink formulation, film optimization, OLEDs fabrication, and transient electroluminescence[J]. *Sci Rep*, 2019, **9**(1): 8493.

[71] Kang Y J, Bail R, Lee C W, et al. Inkjet printing of mixed-host emitting layer for electrophosphorescent organic light-emitting diodes[J]. *ACS Appl Mater Interfaces*, 2019, **11**(24): 21784−21794.

[72] Du Z Z, Liu Y K, Xing X, et al. Inkjet printing multilayer OLEDs

with high efficiency based on the blurred interface[J]. *J Phys D Appl Phys*, 2020, **53**(35): 355105.

[73] Yang P H, Zhang L, Kang D J, et al. High-resolution inkjet printing of quantum dot light-emitting microdiode arrays[J]. *Adv Opt Mater*, 2020, **8**(1): 1901429.

[74] Chen Z X, Li F S, Zeng Q Y, et al. Inkjet-printed pixelated light-emitting electrochemical cells based on cationic Ir(III) complexes[J]. *Org Electron*, 2019, **69**: 336−342.

[75] Yin Y M, Hu Z P, Ali M U, et al. Full-color micro-LED display with $CsPbBr_3$ perovskite and CdSe quantum dots as color conversion layers[J]. *Adv Mater Technol*, 2020, **5**(8): 2000251.

[76] Chen H, Ye F, Tang W T, et al. A solvent-and vacuum-free route to large-area perovskite films for efficient solar modules[J]. *Nature*, 2017, **550**(7674): 92−95.

作者简介

刘士浩 (1992-)，男，博士，副教授，主要从事有机半导体的载流子动力学及发光特性研究。

E-mail：liushihao@jlu.edu.cn

【通信作者】谢文法 (1978-)，男，博士，教授，主要从事有机电子方面的研究。

E-mail：xiewf@jlu.edu.cn

张乐天 (1977-)，女，博士，教授，主要从事有机电致发光器件及其器件物理方面的研究。

E-mail：zlt@jlu.edu.cn

Solution processed organic light-emitting devices: structure, device physics and fabrication process

Liu Shihao, Zhang Letian, Xie Wenfa*

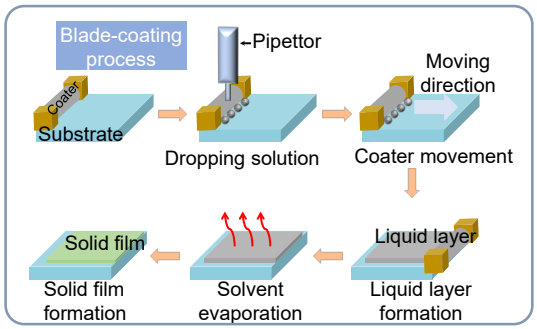

Ultrasonic spray coating process for OLEDs.

Overview: In this paper, we reviewed multilayer structures of the solution-processed organic light-emitting devices (OLEDs), including normal structure, inverted structure, and tandem structure. From a physical point of view, we discussed and summarized that those multilayer structures are important to improve current balance. The improved current balance can reduce internal accumulations of carriers or current leakages, both of which are detrimental to the device's efficiency and lifetime. We also discussed that multilayer structures are necessary to avoid coupling between dipole sources and surface plasmon polariton (SPP) at the metal-dielectric interface. Thus, we concluded that multilayer structures actually play a key role in achieving solution-processed OLEDs with high performances.

Next, we summarized four solution-processing technologies for OLEDs: spin coating process, spray coating process, blade coating process, and inkjet printing process, as well as their problems involved in preparing multilayer structures. Due to self-leveling under centrifugal force, spin-coated films have a huge advantage in film uniformity. With the aid of the orthogonal solvent system and cross-linked material strategy, the spin coating process can prepare multilayer structures. But the two strategies may cause the problems such as carrier trap and accumulation, which would degrade the device's performances. Besides, due to the capillary flow and Marangoni flow, spray coating process, blade coating process, and inkjet printing process require the add of a surfactant or dual solvent systems to prepare uniform films. In addition, the amount of liquid film and its drying rate can be precisely controlled by the blade coating process and inkjet printing process. As a result, solution-processed multilayer structures can be achieved by the two fabrication processes without using the orthogonal solvent system and crosslinking material strategy. But they are still limited by equipment precision and solvent characteristics.

In conclusion, multilayer structures are necessary to achieve high-performance for solution-processed OLEDs. It is demonstrated that the existing solution-processing technologies can prepare multilayer structures for OLEDs. However, due to similar polarities of organic molecules, the existing solution-processing technologies still have problems with the universality of multilayer structures. The advantage of the existing solution-processing technologies with low costs is that it does not rely on high vacuum, and their problems are mainly caused by the use of solvent. In the field of perovskite, Professor Han Liyuan's team developed a new solvent-free and non-vacuum deposition process for the preparation of methyl ammonium halide lead perovskite film, namely, soft pressure processing. This process can not only retain the low-cost advantages of the existing solution-processing technologies, but also avoid the problems caused by the introduction of solvents. Thus, this process could have great potential in the preparation of low-cost multi-layer OLEDs.

Liu S H, Zhang L T, Xie W F. Solution processed organic light-emitting devices: structure, device physics and fabrication process[J]. *Opto-Electron Eng*, 2022, **49**(5): 210407; DOI: 10.12086/oee.2022.210407

Foundation item: National Natural Science Foundation of China (61905086, 62174067, 62175085), and Natural Science Foundation of Jilin Province (20190101024JH, 20200201296JC)

State Key Laboratory of Integrated Optoelectronics, College of Electronic Science and Engineering, Jilin University, Changchun, Jilin 130012, China

* E-mail: xiewf@jlu.edu.cn